MAGNETIC RESONANCE IN CHEMISTRY
Magn. Reson. Chem. 2006; **44**: S51–S60
Published online in Wiley InterScience (www.interscience.wiley.com). DOI: 10.1002/mrc.1817

Principles and applications of GFT projection NMR spectroscopy†

Thomas Szyperski* and Hanudatta S. Atreya

Departments of Chemistry and Structural Biology, The State University of New York at Buffalo, The Northeast Structural Genomics Consortium, Buffalo, NY 14260, USA

Received 2 December 2005; Revised 20 January 2006; Accepted 28 February 2006

The two defining features of G-matrix Fourier transform (GFT) projection NMR spectroscopy are (i) repeated joint sampling of several indirect chemical shift evolution periods of a multidimensional NMR experiment so that transfer amplitudes are generated which are proportional to all possible permutations of cosine and sine modulations of the individual shifts, and (ii) linear combination of the subspectra resulting from such repeated joint sampling in the time or frequency domain which yields edited subspectra containing signals encoding phase-sensitively detected linear combinations of the jointly sampled shifts. This review sketches the underlying principles of GFT NMR and outlines its relation to further developments such as the reconstruction of multidimensional NMR spectra. Copyright © 2006 John Wiley & Sons, Ltd.

KEYWORDS: GFT projection NMR; reduced-dimensionality NMR; projection-reconstruction; rapid NMR data collection; protein structure determination; structural genomics

INTRODUCTION

The speed of multidimensional NMR data acquisition is limited by the need to sample (several) indirect dimensions. This restriction has been termed the 'NMR sampling problem'.[1] Associated with this problem is the 'sampling limited' data collection regime,[2] in which valuable instrument time is invested to meet with the sampling demand and not for achieving sufficient signal-to-noise ratios. G-matrix Fourier transform (GFT) projection NMR spectroscopy[3] allows one to speed up NMR data collection by obtaining high-dimensional spectral information from low-dimensional projections. GFT NMR is thus primarily an approach that enables one to *avoid* sampling-limited data acquisition.

A BRIEF HISTORY OF PROJECTION NMR SPECTROSCOPY

The development of projection NMR spectroscopy until the mid-1980s was reviewed by Ernst *et al*.[4] At that time, the use of 'skewed' projections with a projection angle differing from 0° or 90° was limited to *homo*-nuclear 2D *J*-spectroscopy, and was geared toward obtaining (partially) decoupled projected 1D ^{1}H NMR spectra.[5,6] The 'projection cross-section theorem' was employed to calculate the projected 1D NMR spectra. Importantly, scalar couplings were not detected in a phase-sensitive manner in the indirect dimension of 2D *J*-spectroscopy, so that the NMR signals exhibited both absorptive and dispersive components. This forced researchers[4] to (i) project absolute value spectra,[5] (ii) eliminate dispersive components by use of 'pseudo-echo filtering', (iii) computationally subtract the dispersive component, or (iv) calculate 'skyline projections'. An urgent need for phase-sensitive detection of projected NMR spectra was thus evident early on. In another vein, Ernst and co-workers then introduced 'accordion' NMR spectroscopy,[7] in which the mixing time (serving in 2D exchange spectroscopy (EXSY) to monitor a chemical exchange process) is jointly incremented with the indirect chemical shift evolution period. Considering the mixing time as a third dimension, this approach constitutes a projection technique that is based on a specific protocol to sample the time domain.

In the early 1990s, the co-incrementation of two chemical shift evolution periods was introduced as two-spin coherence spectroscopy[8] and its generalization, reduced-dimensionality (RD) NMR spectroscopy.[9] The RD NMR time domain sampling approach requires that the two nuclei which shall be jointly sampled can be independently excited, and is thus primarily used for projecting multidimensional *hetero*-nuclear *N*-dimensional (*N*D, with $N > 2$) chemical shift correlation spectra into an $N-1$ dimensional subspace. Instead of employing the projection cross-section theorem to calculate the $(N-1)$D projected spectrum from its parent *N*D data set, one of the two jointly sampled *indirect* dimensions is detected in a phase-sensitive manner, while the evolution of the second shift provides a simple cosine modulation of the transfer amplitude. This allows one to phase-sensitively detect a pair of peaks ('chemical shift doublet') located at

*Correspondence to: Thomas Szyperski, Department of Chemistry, The State University of New York at Buffalo, Buffalo, NY 14260, USA. E-mail: szypersk@chem.buffalo.edu
†Dedicated to Gaetano Montelione for his pioneering contributions for NMR-based structural genomics.

the sum and the difference of the two jointly sampled shifts. The angle for the 'projection' can evidently be defined by adjusting the scaling factor for the increments of the two indirect dimensions (Fig. 1).[9–11] Since the time evolution of magnetization due to the build-up of chemical exchange in 2D EXSY differs from the evolution due to chemical shifts in correlation spectroscopy, RD NMR spectroscopy exhibits spectroscopic features that are distinct from accordion NMR spectroscopy.[12–14]

The scope of RD NMR was further expanded by introducing an approach for editing the components of the chemical shift doublet arising from the projection into two subspectra,[15] and, as an alternative, the employment of time proportional phase incrementation (TPPI)[16] to place the components arising from the projection into distinct spectral regions.[11,17] Other innovations that have been introduced until 1998 (see Ref. 1 for a recent review and additional references therein) include (i) the symmetrization of RD NMR spectra to increase signal-to-noise ratios,[11,17,18] (ii) the detection of 'central peaks' located at the center of the two components of the chemical shift doublets in order to restore the full potential of the parent *N*D NMR experiment (corresponding to projection angles of 0° and 90°), and (iii) the twofold application of the RD NMR approach yielding a total of four components resulting from a projection of an *N*D spectrum into an $(N-2)$D space.[19,20]

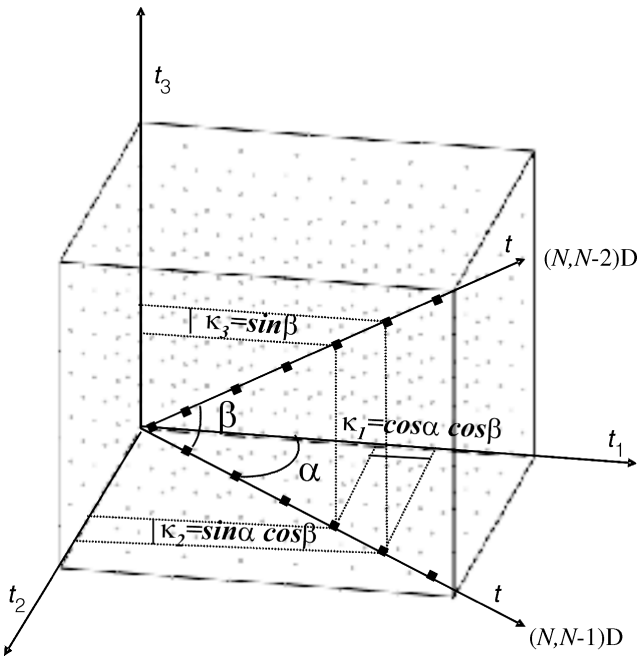

Figure 1. Three-dimensional subspace of an *N*-dimensional NMR experiment. Gray dots indicate data points, which need to be sampled in a conventional FT-NMR experiment, and black squares represent data points acquired 2^K times in a projected NMR experiment with varying sine and cosine modulations of the jointly sampled shifts (see text). The projection tilt angles, which are adjusted by setting the scaling factors (κ) of the individual chemical shift evolution periods, are also indicated.

DEFINING FEATURES OF GFT PROJECTION NMR

Two key features define GFT projection NMR spectroscopy,[3] which represents a generalization of RD NMR. The first is the 2^K-fold repeated joint sampling of K indirect chemical shift evolution periods in conjunction with one evolution period which is detected phase-sensitively and comprises signals at Ω_0, so that the transfer amplitude of each of the 2^K subspectra is proportional to one of the 2^K possible permutations of cosine and sine modulations with the K shifts. The second feature is the generation of linear combinations of the 2^K subspectra, so that each of the 2^K components of the chemical shift multiplets located at $\Omega_0 \pm \Omega_1 \pm \Omega_2 \pm \cdots \pm \Omega_K$ is phase-sensitively detected and edited into separate subspectra each comprising peaks with a given linear combination of shifts. To recover the full potential of the parent multidimensional NMR experiment, bottom-up identification of central peaks (located in projected planes with 0° and 90° tilt angle) can be employed.[3] Including the 2^K 'basic spectra' alluded to above, complete central peak detection requires recording of a total of $2^{K+1}-1$ subspectra, which is the minimal number of subspectra required for resolving arbitrary $N-1$ fold chemical shift degeneracy in a projected *N*D experiment.

G-MATRIX TRANSFORMATION

The 'G-matrix' allows one to linearly combine the 2^K subspectra so that the 2^K components of the shift multiplets are edited into different 2^K subspectra.[3] Hence, the G-matrix represents a generalization of the addition theorems of trigonometric functions. Considering that each of the 2^K subspectra contains a real and an imaginary part, a total of 2^{K+1} data sets is obtained, represented by a 2^{K+1} dimensional vector:

$$\mathbf{S}(K) = \begin{bmatrix} C_K \\ S_K \end{bmatrix} \otimes \cdots \otimes \begin{bmatrix} C_1 \\ S_1 \end{bmatrix} \otimes \begin{bmatrix} C_0 \\ S_0 \end{bmatrix} \qquad (1)$$

with $C_j = \cos(\kappa_j \Omega_j t)$ and $S_j = \sin(\kappa_j \Omega_j t)$. As usual, t represents the evolution time in the indirect GFT dimension where the j-th chemical shift is scaled by a factor, κ_j. When $\mathbf{S}(K)$ is multiplied with the G-matrix according to:

$$\mathbf{T}(K) = \mathbf{G}(K) \cdot \mathbf{S}(K) \qquad (2)$$

one obtains the vector $\mathbf{T}(K)$ comprising the edited subspectra. It is convenient to write $\mathbf{T}(K)$ in complex notation since the imaginary parts of the subspectra are discarded after Fourier transformation. In this case, we have the G-matrix representing a $2^K \times 2^{K+1}$ complex matrix:

$$\mathbf{G}(K) = \begin{bmatrix} 1 & i \\ 1 & -i \end{bmatrix}_1 \otimes \cdots \otimes \begin{bmatrix} 1 & i \\ 1 & -i \end{bmatrix}_K \otimes [1 \quad i] \qquad (3)$$

This can be further illustrated for a three-dimensional subspace projected into a single 'GFT dimension', where Ω_0, Ω_1 and Ω_2 represent the three jointly sampled shifts, i.e. for $K = 2$. The real and imaginary parts of the $2^K = 4$ spectra

Table 1. GFT/G^{2}FT NMR experiments

Research group; Experiment name	Magnetization transfer pathway[a]	Linear combination of chemical shifts observed in the GFT dimension(s) (ω_1/ω_2)
Szyperski and co-workers		
1. Backbone and $^1H^{\beta}/^{13}C^{\beta}$ resonance assignments		
(5,2)D HACACONHN[3]	$^1H^{\alpha}_{i-1}$ (t_1) → $^{13}C^{\alpha}_{i-1}$ (t_1) → $^{13}C'_{i-1}$ (t_1) → $^{15}N_i$ (t_2) → ^1HN_i (t_2)	$\Omega(^{15}N_i) \pm \Omega(^{13}C'_{i-1}) \pm \Omega(^{13}C^{\alpha}_{i-1}) \pm \Omega(^1H^{\alpha}_{i-1})$
(5,3)D HACACONHN[12]	(t_1) (t_1) (t_1) (t_2) (t_3)	$\Omega(^{13}C'_{i-1}) \pm \Omega(^{13}C^{\alpha}_{i-1}) \pm \Omega(^1H^{\alpha}_{i-1})$
(5,2)D HACA, CONHN[12]	$^1H^{\alpha}_{i}$ (t_1) → $^{13}C^{\alpha}_{i}$ (t_1) → $^{13}C'_{i}$ (t_1) → $^{13}C^{\alpha}_{i}$ → $^{15}N_i$ (t_1) → ^1HN_i (t_2)	$\Omega(^{15}N_i) \pm \Omega(^{13}C'_{i}) \pm \Omega(^{13}C^{\alpha}_{i}) \pm \Omega(^1H^{\alpha}_{i})$
(5,3)D HACA, CONHN[12]	(t_1) (t_1) (t_1) (t_2) (t_3)	$\Omega(^{13}C'_{i-1}) \pm \Omega(^{13}C^{\alpha}_{i-1}) \pm \Omega(^1H^{\alpha}_{i-1})$
(4,3)D CBCACONHN[12]	$^1H^{\alpha\beta}_{i-1}$ → $^{13}C^{\alpha\beta}_{i-1}$ (t_1) → $^{13}C^{\alpha}_{i-1}$ → $^{13}C'_{i-1}$ (t_1) → $^{15}N_i$ (t_2) → ^1HN_i (t_3)	$\Omega(^{13}C'_{i-1}) \pm \Omega\,(^{13}C^{\alpha}_{i-1})$; $\Omega(^{13}C'_{i-1}) \pm \Omega(^{13}C^{\beta}_{i-1})$
(4,3)D CBCA, CONHN[12]	$^1H^{\alpha\beta}_{i}$ → $^{13}C^{\alpha\beta}_{i}$ (t_1) → $^{13}C^{\alpha}_{i}$ → $^{13}C'_{i}$ (t_1) → $^{15}N_i$ (t_2) → ^1HN_i (t_3)	$\Omega(^{13}C'_{i}) \pm \Omega\,(^{13}C^{\alpha}_{i})$; $\Omega(^{13}C'_{i}) \pm \Omega(^{13}C^{\beta}_{i})$
(4,3)D HNNC$^{\alpha\beta}$ C$^{\alpha}$13	$^1HN_i \rightarrow {}^{15}N_i \rightarrow {}^{13}C^{\alpha}_{i/i-1}$ (t_1) $\rightarrow {}^{13}C^{\alpha\beta}_{i/i-1}$ (t_1) $\rightarrow {}^{13}C^{\alpha}_{i/i-1}$ (t_2) $\rightarrow {}^{15}N_i \rightarrow {}^1HN_i$ (t_3)	$\Omega(^{13}C^{\alpha}_{i/i-1}) \pm \Omega(^{13}C^{\alpha}_{i/i-1})$; $\Omega(^{13}C^{\alpha}_{i/i-1}) \pm \Omega(^{13}C^{\beta}_{i/i-1})$
(4,3)D HNN(CO)C$^{\alpha\beta}$C$^{\alpha}$13	$^1HN_i \rightarrow {}^{15}N_i \rightarrow {}^{13}C'_{i-1} \rightarrow {}^{13}C^{\alpha}_{i-1} \rightarrow {}^{13}C^{\alpha\beta}_{i-1}$ (t_1) $\rightarrow {}^{13}C^{\alpha}_{i-1}$ (t_1) $\rightarrow {}^{13}C'_{i-1}$ (t_1) $\rightarrow {}^{15}N_i$ (t_2) $\rightarrow {}^1HN_i$ (t_3)	$\Omega(^{13}C^{\alpha}_{i-1}) \pm \Omega(^{13}C^{\alpha}_{i-1})$; $\Omega(^{13}C^{\alpha}_{i-1}) \pm \Omega(^{13}C^{\beta}_{i-1})$
(4,3)D C$^{\alpha\beta}$C$^{\alpha}$ (CO)NHN[13]	$^1H^{\alpha\beta}_{i-1}$ → $^{13}C^{\alpha\beta}_{i-1}$ (t_1) → $^{13}C^{\alpha}_{i-1}$ (t_1) → $^{13}C'_{i-1}$ → $^{15}N_i$ (t_2) → ^1HN_i (t_3)	$\Omega(^{13}C^{\alpha}_{i-1}) \pm \Omega(^{13}C^{\alpha/\beta}_{i-1})$;
(5,3)D H$^{\alpha\beta}$C$^{\alpha\beta}$C$^{\alpha}$ (CO)NHN[13]	(t_1) (t_1) (t_1) (t_2) (t_3)	$\Omega(^{13}C^{\alpha}_{i-1}) \pm \Omega(^{13}C^{\alpha/\beta}_{i-1}) \pm \Omega(^1H^{\alpha/\beta}{}_{i-1})$;
(6,3)D H$^{\alpha\beta}$C$^{\alpha\beta}$C$^{\alpha}$ (CO)NHN[13]	(t_1) (t_1) (t_1) (t_1) (t_2) (t_3)	$\Omega(^{13}C^{\alpha/\beta}_{i-1}) \pm \Omega(^{13}C^{\alpha/\beta}_{i-1}) \pm \Omega(^1H^{\alpha/\beta}_{i-1}) \pm \Omega(^{13}C'_{i-1})$;
2. Side-chain resonance assignments		
(5,3)D HCC-CH[13]	$^1H^{(1)}$ (t_1) → $^{13}C^{(1)}$ (t_1) → $^{13}C^{(2)}$ (t_1) → $^{13}C^{(2)}$ (t_2) → $^1H^{(2)}$ (t_3)	$\Omega(^{13}C^{(2)}) \pm \Omega\,(^{13}C^{(1)}) \pm\Omega\,(^1H^{(1)})$ 'cross peak'; $\Omega\,(^{13}C^{(2)})\pm\Omega\,(^{13}C^{(2)}) \pm \Omega\,(^1H^{(2)})$ 'diagonal peak'
(4,2)D HCCH[13] (aliphatic/aromatic)	$^1H^{(1)}$ (t_1) → $^{13}C^{(1)}$ (t_1) → $^{13}C^{(2)}$ (t_1) → $^1H^{(2)}$ (t_2)	$\Omega(^{13}C^{(2)}) \pm \Omega\,(^{13}C^{(1)}) \pm\Omega\,(^1H^{(1)})$ 'cross peak'; $\Omega\,(^{13}C^{(2)})\pm\Omega\,(^{13}C^{(2)}) \pm \Omega(^1H^{(2)})$ 'diagonal peak'
(4,3)D HCCH[40] (aliphatic/aromatic)	(t_1) (t_1) (t_2) (t_3)	$\Omega(^{13}C^{(1)}) \pm \Omega\,(^1H^{(1)})$ 'cross peak'; $\Omega\,(^{13}C^{(2)}) \pm\Omega\,(^1H^{(2)})$ 'diagonal peak'
L-TROSY-(4,3)D HCCH[41] (aromatic)	$^1H^{(1)}$ (t_1) → $^{13}C^{(1)}$ (t_1) → $^{13}C^{(2)}$ (t_2) → $^1H^{(2)}$ (t_3)	$\Omega\,(^{13}C^{(1)}) \pm\Omega\,(^1H^{(1)})$ 'cross peak'; $\Omega(^{13}C^{(2)}) \pm \Omega(^1H^{(2)})$ 'diagonal peak'
3. GFT NOESY		
(4,3)D [HC^{ali}/HN]−NOESY − CH^{ali}/NH][42]	$^1H^{ali\,(1)} \rightarrow {}^{13}C^{(1)}$; $^1H^{N\,(1)} \rightarrow {}^{15}N^{(1)}$ (t_1) → NOE → $^1H^{ali/1}H^{N\,(1)} \rightarrow {}^1H^{ali\,/\,1}H^{N\,(2)}$ (t_1) → $^{13}C^{(2)} \rightarrow {}^1H^{ali(2)}$; $^{15}N^{(2)} \rightarrow {}^1H^{N(2)}$ (t_2 t_3)	$\Omega(^1H^{ali(1)}) \pm \Omega(^{13}C^{ali(1)})\Omega(^1H^{N(1)}) \pm \Omega(^{15}N^{(1)})$ 'cross peak'; $\Omega(^1H^{ali(2)}) \pm \Omega(^{13}C^{ali(2)})\Omega(^1H^{N(2)}) \pm \Omega(^{15}N^{(2)})$ 'cross peak';

(*continued overleaf*)

Table 1. (*Continued*)

Research group; experiment name	Magnetization transfer pathway[a]	Linear combination of chemical shifts observed in the GFT dimension(s)(ω_1/ω_2)
4. G^{2}FT NMR experiments[38]		
L-(5,3)D HN{N, CO}{$C^{\alpha\beta}C^{\alpha}$}	$^{1}HN_i \rightarrow {}^{15}N_i \rightarrow {}^{13}C^{\alpha}_{i/i-1} \rightarrow {}^{13}C^{\alpha\beta}_{i/i-1} \rightarrow {}^{13}C^{\alpha}_{i/i-1} \rightarrow {}^{15}N_i \rightarrow {}^{1}HN_i$ (t_1) (t_1) (t_2) (t_3); $\rightarrow {}^{13}C'_{i-1}$ (t_2)	ω_1: $\Omega(^{13}C^{\alpha}_{i/i-1}) \pm \Omega(^{13}C^{\alpha}_{i/i-1})$; $\Omega(^{13}C^{\alpha}_{i/i-1}) \pm \Omega(^{13}C^{\beta}_{i/i-1})$ ω_2: $\Omega(^{15}N'_i) \pm \Omega(^{13}C'_{i-1})$
L-(5,3)D HN{NCO}{$C^{\alpha\beta}C^{\alpha}$}	$^{1}HN_i \rightarrow {}^{15}Ni \rightarrow {}^{13}C'_{i-1} \rightarrow {}^{13}C^{\alpha}_{i-1} \rightarrow {}^{13}C^{\alpha\beta}_{i-1}$ (t_1) $\rightarrow {}^{13}C^{\alpha}_{i-1}$ (t_1) $\rightarrow {}^{13}C'_{i-1}$ (t_2) $\rightarrow {}^{15}N_i$ (t_2) $\rightarrow {}^{1}HN_i$ (t_3)	ω_1: $\Omega(^{13}C^{\alpha}_{i-1}) \pm \Omega(^{13}C^{\alpha}_{i-1})$; $\Omega(^{13}C^{\alpha}_{i-1}) \pm \Omega(^{13}C^{\beta}_{i-1})$ ω_2: $\Omega(^{15}N'_i) \pm \Omega(^{13}C'_{i-1})$
(5,3)D {$C^{\alpha\beta}C^{\alpha}$}{CON}HN	$^{1}H^{\alpha\beta}_{i-1}$ (t_1) $\rightarrow {}^{13}C^{\alpha\beta}_{i-1}$ (t_1) $\rightarrow {}^{13}C^{\alpha}_{i-1}$ (t_1) $\rightarrow {}^{13}C'_{i-1}$ (t_2) $\rightarrow {}^{15}N_i$ (t_2) $\rightarrow {}^{1}HN_i$ (t_3)	ω_1: $\Omega(^{13}C^{\alpha}_{i-1}) \pm \Omega(^{13}C^{\alpha}_{i-1})$; ω_2: $\Omega(^{15}N'_i) \pm \Omega(^{13}C'_{i-1})$
(6,3)D {$H^{\alpha\beta}C^{\alpha\beta}C^{\alpha}$}{CON}HN	(t_1) (t_1) (t_1) (t_2) (t_2) (t_3)	ω_1: $\Omega(^{13}C^{\alpha}_{i-1}) \pm \Omega(^{13}C^{\alpha/\beta}_{i-1}); \pm\Omega(^{1}H^{\alpha/\beta}_{i-1})$; ω_2: $\Omega(^{15}N'_i) \pm \Omega(^{13}C'_{i-1})$
(5,3)D HN{N, CO}{$C^{\alpha}H^{\alpha}$}	$^{1}HN_i \rightarrow {}^{15}N_i \rightarrow {}^{13}C^{\alpha}_{i/i-1} \rightarrow {}^{1}H^{\alpha}_{i/i-1} \rightarrow {}^{13}C^{\alpha}_{i/i-1} \rightarrow {}^{15}N_i \rightarrow {}^{1}HN_i$ (t_1) (t_1) (t_2) (t_3); $\rightarrow {}^{13}C'_{i-1}$ (t_2)	ω_1: $\Omega(^{13}C^{\alpha}_{i/i-1}) \pm \Omega(^{1}H^{\alpha}_{i/i-1})$; ω_2: $\Omega(^{15}N'_i) \pm \Omega(^{13}C'_{i-1})$
(5,3)D {$H^{\alpha}C^{\alpha}$}{CON}HN	$^{1}H^{\alpha}_{i-1}$ (t_1) $\rightarrow {}^{13}C^{\alpha}_{i-1}$ (t_1) $\rightarrow {}^{13}C'_{i-1}$ (t_2) $\rightarrow {}^{15}N_i$ (t_2) $\rightarrow {}^{1}HN_i$ (t_3)	ω_1: $\Omega(^{13}C^{\alpha}_{i-1}) \pm \Omega(^{13}H^{\alpha}_{i-1})$; ω_2: $\Omega(^{15}N'_i) \pm \Omega(^{13}C'_{i-1})$
L-(5,3)D HN{N, C^{α}}{$C^{\alpha\beta}C^{\alpha}$}	$^{1}HN_i \rightarrow {}^{15}N_i \rightarrow {}^{13}C^{\alpha}_{i/i-1}$ (t_2) $\rightarrow {}^{13}C^{\alpha\beta}_{i/i-1}$ (t_1) $\rightarrow {}^{13}C^{\alpha}_{i/i-1}$ (t_1) $\rightarrow {}^{15}N_i$ (t_2) $\rightarrow$ $^{1}HN_i$ (t_3)	ω_1: $\Omega(^{13}C^{\alpha}_{i/i-1}) \pm \Omega(^{13}C^{\alpha}_{i/i-1})$; $\Omega(^{13}C^{\alpha}_{i/i-1}) \pm \Omega(^{13}C^{\beta}_{i/i-1})$ ω_2: $\Omega(^{15}N'_i) \pm \Omega(^{13}C^{\alpha}_{i})$
L-(5,3)D HN{N(CO)C^{α}}{$C^{\alpha\beta}C^{\alpha}$}	$^{1}HN_i \rightarrow {}^{15}N_i \rightarrow {}^{13}C'_{i-1} \rightarrow {}^{13}C^{\alpha}_{i-1}$ (t_2) $\rightarrow {}^{13}C^{\alpha\beta}_{i-1}$ (t_1) $\rightarrow {}^{13}C^{\alpha}_{i-1}$ (t_1) $\rightarrow {}^{13}C'_{i-1}$ (t_2) $\rightarrow {}^{15}N_i$ (t_2) $\rightarrow {}^{1}HN_i$ (t_3)	ω_1: $\Omega(^{13}C^{\alpha}_{i-1}) \pm \Omega(^{13}C^{\alpha}_{i-1})$; $\Omega(^{13}C^{\alpha}_{i-1}) \pm \Omega(^{13}C^{\beta}_{i-1})$ ω_2: $\Omega(^{15}N'_i) \pm \Omega(^{13}C'_{i-1})$
Gao and co-workers[43]		
1. Backbone and $^{13}C^{\beta}$ resonance assignments		
(3,2)D HNNCO[32]	$^{1}HN_i \rightarrow {}^{15}N_i \rightarrow {}^{13}C'_{i-1}$ (t_1) $\rightarrow {}^{15}N_i$ (t_1) $\rightarrow {}^{1}HN_i$ (t_2)	$\Omega(^{15}N_i) \pm \Omega(^{13}C'_{i-1})$
(3,2)D HNNCA	$^{1}HN_i \rightarrow {}^{15}N_i \rightarrow {}^{13}C^{\alpha}_{i/i-1}$ (t_1) $\rightarrow {}^{15}N_i$ (t_1) $\rightarrow {}^{1}HN_i$ (t_2)	$\Omega(^{15}N_i) \pm \Omega(^{13}C^{\alpha}_{i/i-1})$
(3,2)D HNNCACB	$^{1}HN_i \rightarrow {}^{15}N_i \rightarrow {}^{13}C^{\alpha}_{i/i-1} \rightarrow {}^{13}C^{\alpha\beta}_{i/i-1}$ (t_1) $\rightarrow {}^{13}C^{\alpha}_{i/i-1} \rightarrow {}^{15}N_i$ (t_1) $\rightarrow$ $^{1}HN_i$ (t_2)	$\Omega(^{15}N_i) \pm \Omega(^{13}C^{\alpha}_{i/i-1})/\Omega(^{13}C^{\beta}_{i/i-1})$
(3,2)D HNN(CO)CA	$^{1}HN_i \rightarrow {}^{15}N_i \rightarrow {}^{13}C'_{i-1} \rightarrow {}^{13}C^{\alpha}_{i-1}$ (t_1) $\rightarrow {}^{13}C'_{i-1} \rightarrow {}^{15}N_i$ (t_1) $\rightarrow$ $^{1}HN_i$ (t_2)	$\Omega(^{15}N_i) \pm \Omega(^{13}C^{\alpha}_{i-1})$
(3,2)D HNN(CA)CO	$^{1}HN_i \rightarrow {}^{15}N_i \rightarrow {}^{13}C^{\alpha}_{i} \rightarrow {}^{13}C'_{i}$ (t_1) $\rightarrow {}^{13}C^{\alpha}_{i} \rightarrow {}^{15}N_i$ (t_1) $\rightarrow {}^{1}HN_i$ (t_2)	$\Omega(^{15}N_i) \pm \Omega(^{13}C'i)$
(3,2)D HNN(CO)CACB	$^{1}HN_i \rightarrow {}^{15}N_i \rightarrow {}^{13}C'_{i-1} \rightarrow {}^{13}C^{\alpha}_{i-1} \rightarrow {}^{13}C^{\alpha\beta}_{i-1}$ (t_1) $\rightarrow {}^{13}C^{\alpha}_{i-1} \rightarrow$ $^{13}C'_{i-1} \rightarrow {}^{15}N_i$ (t_1) $\rightarrow {}^{1}HN_i$ (t_2)	$\Omega(^{15}N_i) \pm \Omega(^{13}C^{\alpha}_{i-1})/\Omega(^{13}C^{\beta}_{i-1})$
(3,2)D CBCANHN	$^{1}H^{\alpha\beta}_{i/i-1} \rightarrow {}^{13}C^{\alpha\beta}_{i/i-1}$ (t_1) $\rightarrow {}^{13}C^{\alpha}_{i/i-1} \rightarrow {}^{15}N_i$ (t_2) $\rightarrow {}^{1}HN_i$ (t_1)	$\Omega(^{15}N_i) \pm \Omega(^{13}C^{\alpha}_{i/i-1})/\Omega(^{13}C^{\beta}_{i/i-1})$

Table 1. (*Continued*)

Research group; experiment name	Magnetization transfer pathway[a]	Linear combination of chemical shifts observed in the GFT dimension(s) (ω_1/ω_2)
(3,2)D CBCA(CO)NHN	$^{1}H^{\alpha\beta}_{i-1} \rightarrow {}^{13}C^{\alpha\beta}_{i-1} \rightarrow {}^{13}C^{\alpha}_{i-1} \rightarrow {}^{13}C'_{i-1} \rightarrow {}^{15}N_i \rightarrow {}^{1}HN_i$ (t_1) (t_2) (t_1)	$\Omega(^{15}N_i) \pm \Omega(^{13}C^{\alpha}_{i-1})/\Omega(^{13}C^{\beta}_{i-1})$
2. Side-chain resonance assignments		
(3,2)D C(CCO)NHN	$^{1}H_{i-1} \xrightarrow{\text{TOCSY}} {}^{13}C_{i-1} \rightarrow {}^{13}C_{i-1} \rightarrow {}^{15}N_i \rightarrow {}^{1}HN_i$ (t_1) (t_1) (t_2)	$\Omega(^{15}N_i) \pm \Omega(^{13}C_{i-1})$
(3,2)D H(CCCO)NHN	$^{1}H_{i-1} \xrightarrow{\text{TOCSY}} {}^{13}C_{i-1} \rightarrow {}^{13}C'_{i-1} \rightarrow {}^{15}N_i \rightarrow {}^{1}HN_i$ (t_1) (t_1) (t_2)	$\Omega(^{15}N_i) \pm \Omega(^{1}H_{i-1})$

[a] The labels, t_1, t_2, t_3, refer to frequency labeling of the corresponding nuclei during the chemical shift evolution periods in the 2D/3D experiment.

are denoted S_{jr} and S_{ji} ($j = 1 \cdots 4$) and are proportional to:

$$
\begin{aligned}
S_{1r} &\propto \cos(\kappa_0\Omega_0 t) \times \cos(\kappa_1\Omega_1 t) \times \cos(\kappa_2\Omega_2\, t)\\
S_{1i} &\propto \sin(\kappa_0\Omega_0 t) \times \cos(\kappa_1\Omega_1 t) \times \cos(\kappa_2\Omega_2\, t)\\
S_{2r} &\propto \cos(\kappa_0\Omega_0 t) \times \sin(\kappa_1\Omega_1 t) \times \cos(\kappa_2\Omega_2\, t)\\
S_{2i} &\propto \sin(\kappa_0\Omega_0 t) \times \sin(\kappa_1\Omega_1 t) \times \cos(\kappa_2\Omega_2\, t)\\
S_{3r} &\propto \cos(\kappa_0\Omega_0 t) \times \cos(\kappa_1\Omega_1 t) \times \sin(\kappa_2\Omega_2\, t)\\
S_{3i} &\propto \sin(\kappa_0\Omega_0 t) \times \cos(\kappa_1\Omega_1 t) \times \sin(\kappa_2\Omega_2\, t)\\
S_{4r} &\propto \cos(\kappa_0\Omega_0 t) \times \sin(\kappa_1\Omega_1 t) \times \sin(\kappa_2\Omega_2\, t)\\
S_{4i} &\propto \sin(\kappa_0\Omega_0 t) \times \sin(\kappa_1\Omega_1 t) \times \sin(\kappa_2\Omega_2 t),
\end{aligned}
$$

so that the vector $\mathbf{T}(2) = \mathbf{G}(2) \cdot \mathbf{S}(2)$ is given in complex notation by:

$$
\begin{aligned}
\mathbf{T}(2) &= \begin{bmatrix} e^{i(\kappa_0\times\Omega_0+\kappa_1\times\Omega_1+\kappa_2\times\Omega_2)t} \\ e^{i(\kappa_0\times\Omega_0-\kappa_1\times\Omega_1+\kappa_2\times\Omega_2)t} \\ e^{i(\kappa_0\times\Omega_0+\kappa_1\times\Omega_1-\kappa_2\times\Omega_2)t} \\ e^{i(\kappa_0\times\Omega_0-\kappa_1\times\Omega_1-\kappa_2\times\Omega_2)t} \end{bmatrix} \\
&= \begin{bmatrix} 1 & i & i & -1 & i & -1 & -1 & -i \\ 1 & i & -i & 1 & i & -1 & 1 & i \\ 1 & i & i & -1 & -i & 1 & 1 & i \\ 1 & i & -i & 1 & -i & 1 & -1 & -i \end{bmatrix} \cdot \begin{bmatrix} S_{1r} \\ S_{1i} \\ S_{2r} \\ S_{2i} \\ S_{3r} \\ S_{3i} \\ S_{4r} \\ S_{4i} \end{bmatrix}
\end{aligned} \qquad (4)
$$

Hence, the four linear combinations of chemical shifts, $\kappa_0 \times \Omega_0 \pm \kappa_1 \times \Omega_1 \pm \kappa_2 \times \Omega_2$, are measured in one of the four subspectra each.

GFT NMR data processing and analysis

The free induction decays (FIDs) of the 2^K subspectra constituting $\mathbf{S}(K)$ (Eqn (1)) are routinely recorded in an 'interleaved manner' as a single data set. The subsequent **G**-matrix transformations (Eqn (2)) are carried out with software yielding the subspectra, $\mathbf{T}(K)$, which are then conventionally processed using software packages such as PROSA[21] or NMRPipe.[22]

Data analysis of the GFT NMR subspectra is performed as for 'conventional' spectra, except that one correlates linear combinations of chemical shifts instead of the chemical shifts themselves. Importantly, the **G**-matrix transformation ensures that all linear combinations of shifts that are of the same type are edited into the same subspectra, and that the number of peaks in each of the GFT subspectra is identical to the number in the conventional congeners of same dimensionality. Concomitantly, the spectral dispersion increases since signals are dispersed over the sum of spectral widths. In our laboratory, XEASY,[23] and CARA,[24] both of which allow one to handle linear combination of chemical shifts, are used for analysis of GFT NMR spectra. Once the position of peaks in the spectra encoding the linear of combination of chemical shifts is known, the shifts of individual nuclei within the shift multiplet can be obtained using the linear least-square procedure described previously.[3]

Furthermore, GFT NMR experiments are highly amenable to automated analysis. Firstly, chemical shifts are measured with higher precision and accuracy than in their conventional congeners.[3,12,13] Secondly, detection of peak patterns allows one to identify signals that are closer to the noise level.[3,12] The program AUTOASSIGN[25] is routinely used in our laboratory for protein backbone assignments using chemical shifts derived from GFT NMR spectra.

Sensitivity considerations

Whenever chemical shifts detected in a constant-time manner are jointly sampled, line widths are not affected by the joint sampling but are determined by the maximum evolution time of the constant-time evolution.[3] However, the sensitivity of an (N, $N-K$)D GFT experiment is reduced by a factor of $(1/\sqrt{2})^K$ compared to the parent ND experiment for the same total measurement time. This is because each additional frequency labeling results in a twofold decrease in sensitivity, while a factor of $\sqrt{2}$ is gained owing to the fact that phase-sensitive detection for one shift is omitted. This loss in intrinsic sensitivity can be at least partially recovered by symmetrization[11,17,18,26] of subspectra about the position of

Table 2. Translation of projection (reconstruction) NMR experiments to GFT NMR nomenclature

Research group; projection NMR experiments (with tilt angles)	Equivalent GFT NMR experiment(s)[a] (with corresponding scaling factors)
Marion and co-workers	
1. 3D $^{13}C/^{15}N$ filtered NOESY[15]	(4,3)D [H$\underline{C}^{ali}$]-NOESY-[$\underline{N}$H]
Kozminski and co-workers	
1. 2D RD-H$\underline{N}$C$\underline{A}$[44]	(3,2)D HN$\underline{N}$C$\underline{A}$
2. 2D RD-H$\underline{N}$(CO)C$\underline{A}$[44]	(3,2)D HN$\underline{N}$(CO)C$\underline{A}$
3. 2D RD-H$\underline{A}$C$\underline{A}$N$\underline{H}$[44]	(4,2)D H$\underline{A}$C$\underline{A}$N$\underline{H}$
4. 2D DQ-H$\underline{N}$C$\underline{A}$C$\underline{B}$[45]	(4,2)D HN$\underline{N}$C$^{\alpha\beta}$C$^{\alpha}$
5. 2D DQ-H$\underline{N}$(CO)C$\underline{A}$C$\underline{B}$[45]	(4,2)D HN$\underline{N}$(CO)C$^{\alpha\beta}$C$^{\alpha}$
6. 2D H$\underline{N}$C$\underline{O}$[46]	(3,2)D HN$\underline{N}$C$\underline{O}$
7. 2D H$\underline{N}$C$\underline{A}$[46]	(3,2)D HN$\underline{N}$C$\underline{A}$
8. 2D H$\underline{N}$(CO)C$\underline{A}$[46]	(3,2)D HN$\underline{N}$(CO)C$\underline{A}$
9. 2D H(N)C$\underline{O}$C$\underline{A}$[46]	(3,2)D HN(N)C$\underline{O}$C$\underline{A}$
Brutscher and co-workers	
1. 2D DQ/ZQ HNCA[47]	(3,2)D HN$\underline{N}$C$\underline{A}$
2. 2D DQ/ZQ HN(CO)CA[47]	(3,2)D HN$\underline{N}$(CO)C$\underline{A}$
3. 2D DQ/ZQ HNCACB[47]	(3,2)D HN$\underline{N}$C$^{\alpha\beta}$C$^{\alpha}$
4. 2D DQ/ZQ HN(COCA)CB[47]	(3,2)D HN$\underline{N}$(COCA)C$\underline{B}$
5. 2D DQ/ZQ HN(CA)HA[47]	(3,2)D HN$\underline{N}$(CA)H$\underline{A}$
6. 2D DQ/ZQ HN(COCA)HA[47]	(3,2)D HN$\underline{N}$(COCA)H$\underline{A}$
Kupce and Freeman	
1. 3D HNCO[27]	1. (3,2)D HN$\underline{N}$C$\underline{O}$
Tilt angles: $\alpha = 30^{\circ}$	Scaling factors (κ): N = 0.5;CO = 0.87
Tilt angles: $\alpha = 0^{\circ}, 90^{\circ}$	2D [$^{13}C'$, ^{1}H] Projection of 3D HNNCO, 2D [^{15}N, ^{1}H] HSQC
2. 3D HNCA[28]	2. (3,2)D HN$\underline{N}$C$\underline{A}$
Tilt angles: $\alpha = \pm 30^{\circ}$	Scaling factors (κ): N = 0.5; CA = 0.87
Tilt angles: $\alpha = 0^{\circ}, 90^{\circ}$	2D [$^{13}C'$, ^{1}H] Projection of 3D HNNCA, 2D [^{15}N, ^{1}H] HSQC
3. 3D HN(CO)CA[28]	3. (3,2)D HN$\underline{N}$(CO)C$\underline{A}$
Tilt angles: $\alpha = \pm 60^{\circ}$	Scaling factors (κ): N = 0.87; CA = 0.5
Tilt angles: $\alpha = 0^{\circ}, 90^{\circ}$	2D [$^{13}C'$, ^{1}H] Projection of 3D HNN(CO)CA, 2D [^{15}N, ^{1}H] HSQC
4. 4D HNCOCA[30]	4. (4,2)D HN$\underline{N}$C$\underline{O}$C$\underline{A}$
Tilt angles: $\alpha = \pm 45^{\circ}$; $\beta = \pm 45^{\circ}$	Scaling factors (κ): N = 0.71; CO = 0.5; CA = 0.5
Tilt angles: $\alpha = 0^{\circ}$; $\beta = 0^{\circ}$	2D [$^{13}C'$, ^{1}H] Projection of 4D HNNCOCA
$\alpha = 90^{\circ}$; $\beta = 0^{\circ}$	2D [$^{13}C^{\alpha}$, ^{1}H] Projection of 4D HNNCOCA
$\alpha = 0^{\circ}$; $\beta = 90^{\circ}$	2D [^{15}N, ^{1}H] HSQC
5. The 'TILT' experiment: 3D ^{15}N-NOESY-HSQC and ^{15}N-TOCSY-HSQC[48]	5. (3,2)D [$\underline{H}$]-NOESY-[$\underline{N}$H]/(3,2)D [$\underline{H}$]-TOCSY-[$\underline{N}$H]
Tilt angle: $\alpha = 0^{\circ}$,	Scaling factors (κ): H = 1.0, N = 0.0
$\alpha = \pm 30^{\circ}$	H = 0.87, N = 0.5
Zhou and co-workers	
1. 5-D HACACONH[33]	1. (5,2)D H$\underline{A}$C$\underline{A}$C$\underline{O}$N$\underline{H}$N
Tilt angles:	Scaling factor (κ):
N = ±60, CO = ±60, CA = ±60, HA = ±60	N = 0.5, CO = 0.5, CA = 0.5, HA = 0.5
Tilt angles:	
N = 0°, CO = 90°, CA = 90°, HA = 90°	2D [^{15}N, ^{1}H] HSQC
N = 90°, CO = 0° CA = 90°, HA = 90°	2D [$^{13}C'$, ^{1}H] projection of 4D/5D HACACONHN
N = 90°, CO = 90° CA = 0°, HA = 90°	2D [$^{13}C^{\alpha}$, ^{1}H] projection of 4D/5D HACACONHN
N = 90°, CO = 90° CA = 90°, HA = 0°	2D [$^{1}H^{\alpha}$, ^{1}H] projection of 4D/5D HACACONHN

Table 2. (*Continued*)

Research group; projection NMR experiments (with tilt angles)	Equivalent GFT NMR experiment(s)[a] (with corresponding scaling factors)
2. (4,2)D PR-HNCACB[34] Tilt angles: N = 86.0°, CA = 15.5°, CB = 75.0° N = 73.9°, CA = 33.7°, CB = 61.3° N = 54.7°, CA = 54.7°, CB = 54.7° N = 33.7°, CA = 73.9°, CB = 61.3° N = 15.5°, CA = 86.0°, CB = 75.0°	2. (4,2)D HN<u>NC</u>$^{\alpha\beta}$<u>C</u>$^{\alpha}$ Scaling factors (κ): N = 0.07, C^{α} = 0.96, C^{β} = 0.26 N = 0.28, C^{α} = 0.83, C^{β} = 0.48 N = 0.58,C^{α} = 0.58, C^{β} = 0.58 N = 0.83, C^{α} = 0.28, C^{β} = 0.48 N = 0.96, C^{α} = 0.07, C^{β} = 0.26
Tilt angles: N = 0°, CA = 90°, CB = 90° N = 90°, CA = 0°, CB = 90° N = 90°, CA = 90°, CB = 0°	2D [^{15}N, ^{1}H] HSQC 2D [$^{13}C^{\alpha}$, ^{1}H] Projection of 3D/4D HNNCACB 2D [$^{13}C^{\beta}$, ^{1}H] Projection of 4D HNNCACB
3. (4,2)D PR-HN(CO)CACB[34] Tilt angles same as in (2)	3. (4,2)D HN<u>N</u>(CO)<u>C</u>$^{\alpha\beta}$<u>C</u>$^{\alpha}$ Scaling factors same as in (2)
4. (4,2)D PR-Intra-HNCACB[34] Tilt angles same as in (2)	4. (4,2)D Intra-HN<u>NC</u>$^{\alpha\beta}$<u>C</u>$^{\alpha}$ Scaling factors same as in (2)
5. (4,2)D PR-HNCACO[34] Tilt angles same as in (2) with CB shift evolution replaced by CO	5. (4,2)D intra-HN<u>NCACO</u> Scaling factors same as in (2) with C^{β} shift evolution replaced by CO
6. (4,2)D PR-HNCOCA[34] Tilt angles same as in (2) with CA Shift evolution replaced by CO and CB Shift evolution replaced by CA	6. (4,2)D HN<u>NCOCA</u> Scaling factors same as in (2) with C^{α} replaced by CO and C^{β} replaced by CA
7. (4,2)D PR-HNCO$_{i-1}$CA$_i$[34] Tilt angles same as in (2) with CA shift evolution replaced by CO and CB shift evolution replaced by CA	7. (4,2)D HN<u>N</u><<u>CO</u>,<u>CA</u>> Scaling factors same as in (2) with C^{α} shift evolution replaced by CO and C^{β} shift evolution replaced by CA
8. (4,2)D PR-HACANH[34] Tilt angles same as in (2) with CA shift evolution replaced by HA and CB shift evolution replaced by CA	8. (4,2)D <u>HACAN</u>HN Scaling Factors same as in (2) with C^{α} shift evolution replaced by HA and C^{β} shift evolution replaced by CA
9. (4,2)D PR-HACA(CO)NH[34] Tilt angles same as in (2) with CA shift evolution replaced by HA and CB shift evolution replaced by CA	9. (4,2)D <u>HACA</u>(CO)<u>N</u>H Tilt angles same as in (2) with CA shift evolution replaced by HA and CB shift evolution replaced by CA
10. (4,2)D PR CH_3-N NOESY[49] Tilt angles: 100 Projection angles distributed evenly in angle space: N = α_i; H = β_i; C = γ_i; i = 1.100	10. (4,2)D [<u>HC</u>^{ali}]-NOESY-[<u>N</u>H] Scaling factors (κ): N = cos(α_i), H = cos(β_i), C^{ali} = cos(γ_i); i = 1.100
11. (4,3)D HC(CO)NH-TOCSY and (4,3)D HC(C)NH-TOCSY[50] Tilt angles: α = 0°, ±18°, ±36°, ±54°, ±72°, 90°	11. (4,3)D <u>HC</u>(CO)NH-TOCSY and (4,3)D <u>HC</u>(C)NH-TOCSY Scaling factors (κ): ^{1}H = 1.0, 0.95, 0.81, 0.58, 0.31, 0.0 ^{13}C = 0.0, 0.31, 0.58, 0.81, 0.95, 1.0
Wüthrich and co-workers[51]	
1. 4D APSY-HNCOCA Tilt angles: $\alpha = \pm 30°$; $\beta = 0°$ $\alpha = \pm 60°$; $\beta = 0°$ Tilt angles: $\alpha = 0°$; $\beta = \pm 30°$ $\alpha = 0°$; $\beta = \pm 60°$	1. Set of (3,2)D and (4,2)D GFT NMR experiments: (3,2)D HN(N)<u>COCA</u> Scaling factors (κ): CO = 0.5; CA = 0.87; CO = 0.87; CA = 0.5 (3,2)D HN<u>N</u>(CO)<u>CA</u> Scaling factors (κ): N = 0.5; CA = 0.87 N = 0.87; CA = 0.5

(*continued overleaf*)

Table 2. (*Continued*)

Research group; projection NMR experiments (with tilt angles)	Equivalent GFT NMR experiment(s)[a] (with corresponding scaling factors)
	(3,2)D HN<u>NCO</u>
Tilt angles: $\alpha = 90°; \beta = \pm 30°$	Scaling factors (κ): N = 0.5; CO = 0.87
$\alpha = 90°; \beta = \pm 60°$	N = 0.87; CO = 0.5
	(4,2)D HN<u>NCOCA</u>
Tilt angles: $\alpha = \pm 30°; \beta = \pm 30°$	Scaling factors (κ): N = 0.5; CO = 0.44; CA = 0.75
$\alpha = \pm 60°; \beta = \pm 30°$	N = 0.5; CO = 0.75; CA = 0.44
$\alpha = \pm 45°; \beta = \pm 60°$	N = 0.87; CO = 0.35; CA = 0.35
Tilt angles: $\alpha = 0°; \beta = 0°$	2D [$^{13}C^{\alpha}$, ^{1}H] Projection of 4D HNNCOCA
$\alpha = 90°; \beta = 0°$	2D [$^{13}C'$, ^{1}H] Projection of 4D HNNCOCA
$\alpha = 0°; \beta = 90°$	2D [^{15}N, ^{1}H] HSQC
2. 5D APSY-HACACONH	2. A set of (3,2)D GFT NMR experiments
	(3,2)D (HACA)<u>CON</u>HN
Tilt angles: $\alpha = \pm 30°; \beta = 0°; \gamma = 0°$	Scaling factors (κ): N = 0.87; CO = 0.5
$\alpha = \pm 60°; \beta = 0°; \gamma = 0°$	Scaling factors (κ): N = 0.5; CO = 0.87
	(3,2)D (HA)<u>CA</u>(CO)<u>N</u>HN
Tilt angles: $\alpha = 0°; \beta = \pm 30°; \gamma = 0°$	Scaling factors (κ): N = 0.87; CA = 0.5
$\alpha = 0°; \beta = \pm 60°; \gamma = 0°$	N = 0.5; CA = 0.87
	(3,2)D <u>HA</u>(CACO)<u>N</u>HN
Tilt angles: $\alpha = 0°; \beta = 0°; \gamma = \pm 30°$	Scaling factors (κ): N = 0.87; HA = 0.5
$\alpha = 0°; \beta = 0°; \gamma = \pm 60°$	N = 0.5; HA = 0.87
	(3,2)D (HA)<u>CACO</u>(N)HN
Tilt angles: $\alpha = 90°; \beta = \pm 30°; \gamma = 0°$	Scaling factors (κ): CA = 0.5; CO = 0.87
$\alpha = 90°; \beta = \pm 60°; \gamma = 0°$	CA = 0.87; CO = 0.5
	(3,2)D <u>HA</u>(CA)<u>CO</u>(N)HN
Tilt angles: $\alpha = 90°; \beta = 0°; \gamma = \pm 30°$	Scaling factors (κ): CO = 0.87; HA = 0.5
$\alpha = 90°; \beta = 0°; \gamma = \pm 60°$	CO = 0.5; HA = 0.87
	(3,2)D <u>HACA</u>(CON)HN
Tilt angles: $\alpha = 0°; \beta = 90°; \gamma = \pm 30°$	Scaling factors (κ): CA = 0.87; HA = 0.5
$\alpha = 0°; \beta = 90°; \gamma = \pm 60°$	CA = 0.5; HA = 0.87
Tilt angles: $\alpha = 0°; \beta = 0°; \gamma = 0°$	2D [^{15}N, ^{1}H] HSQC
$\alpha = 90°; \beta = 0°; \gamma = 0°$	2D [$^{13}C'$, ^{1}H] Projection of 4D HNNCOCA
$\alpha = 0°; \beta = 90°; \gamma = 0°$	2D [$^{13}C^{\alpha}$, ^{1}H] Projection of 4D HNNCOCA
$\alpha = 0°; \beta = 0°; \gamma = 90°$	2D [$^{1}H^{\alpha}$, ^{1}H] Projection of 4D/5D HACACONHN
Wagner and co-workers[52]	
3D RD-HCcoNH-TOCSY	(4,3)D <u>HC</u>(CO)NHN-TOCSY
Markley and co-workers[37]	
1. 3D HNCO[b]	1. (3,2)D HN<u>NCO</u>
Tilt angles: $\alpha = 50°, 35°, 10°, 70°, 20°, 25°, 45°$	Scaling factors (κ): N = 0.76, 0.57, 0.17, 0.94, 0.34, 0.42, 0.71
	CO = 0.64, 0.82, 0.98, 0.34, 0.94, 0.90, 0.71
2. 3D HNCACB[b]	2. (3,2)D HN<u>NCACB</u>
Tilt angles: $\alpha = 20°, 10°, 30°, 40°, 50°, 60°, 70°$	Scaling factors (κ): N = 0.34, 0.17, 0.50, 0.64, 0.76, 0.87, 0.94
	CA/CB = 0.94, 0.98, 0.87, 0.76, 0.64, 0.50, 0.34
3. 3D CBCA(CO)NHN[b]	3. (3,2)D <u>CBCA</u>(CO)<u>N</u>HN
Tilt angles: $\alpha = 50°, 55°, 40°, 70°, 30°, 65°, 20°$	Scaling factors (κ): N = 0.76, 0.82, 0.65, 0.94, 0.87, 0.90, 0.34
	CA/CB = 0.64, 0.57, 0.76, 0.34, 0.50, 0.42, 0.94

[a] Only basic spectra are considered, unless otherwise indicated.

[b] The tilt angles for mouse protein Mm202773 are considered.[37]

central peaks,[3] and an increase in sensitivity by a factor of about $\sqrt{2^K}$ can be expected for an $(N, N-K)$D GFT experiment in case the symmetrization is performed in a bottom-up manner.[3,12]

FURTHER DEVELOPMENTS

Projection-reconstruction NMR spectroscopy

Kupce and Freeman proposed the use of GFT NMR subspectra for the reconstruction of the multidimensional parent spectrum, taking advantage of the option to scale the jointly sampled chemical shifts.[27–30] For that purpose, the GFT NMR formalism was translated into a form that is more readily related to the terminology used in projection-reconstruction (PR) theory.[31,32] In particular, the **G**-matrix transformation was referred to as a (generalized) 'hypercomplex FT' of tilted planes in projected NMR experiments. For $K = 2$, we compare Eqn (4) with Eqn (S14) of Ref. 30

$$s_{+\alpha,+\beta} = 0.25[(s_{rrr} - s_{rjk} - s_{ijr} - s_{irk}) + i(s_{irr} - s_{ijk} + s_{rjr} + s_{rrk})]$$

$$s_{+\alpha,-\beta} = 0.25[(s_{rrr} + s_{rjk} - s_{ijr} + s_{irk}) + i(s_{irr} + s_{ijk} + s_{rjr} - s_{rrk})]$$

$$s_{-\alpha,+\beta} = 0.25[(s_{rrr} + s_{rjk} + s_{ijr} - s_{irk}) + i(s_{irr} + s_{ijk} - s_{rjr} + s_{rrk})]$$

$$s_{-\alpha,-\beta} = 0.25[(s_{rrr} - s_{rjk} + s_{ijr} + s_{irk}) + i(s_{irr} - s_{ijk} - s_{rjr} - s_{rrk})]$$

The equivalence of **G**-matrix Eqn (4) with this system of equations becomes readily apparent when considering the correspondence of the following parameters and expressions:

$$s_{+\alpha,+\beta} \leftrightarrow e^{i(\kappa_0\times\Omega_0+\kappa_1\times\Omega_1+\kappa_2\times\Omega_2)t}, s_{+\alpha,-\beta} \leftrightarrow e^{i(\kappa_0\times\Omega_0-\kappa_1\times\Omega_1+\kappa_2\times\Omega_2)t},$$

$$s_{-\alpha,+\beta} \leftrightarrow e^{i(\kappa_0\times\Omega_0+\kappa_1\times\Omega_1-\kappa_2\times\Omega_2)t}, s_{+\alpha,+\beta} \leftrightarrow e^{i(\kappa_0\times\Omega_0-\kappa_1\times\Omega_1-\kappa_2\times\Omega_2)t},$$

and

$$s_{rrr} \leftrightarrow S_{1r}, s_{rjk} \leftrightarrow S_{4r}, s_{ijr} \leftrightarrow S_{3i}, s_{irk} \leftrightarrow S_{2i},$$

$$s_{irr} \leftrightarrow S_{1i}, s_{ijk} \leftrightarrow S_{4i}, s_{rjr} \leftrightarrow S_{3r}, s_{rrk} \leftrightarrow S_{2r}.$$

Moreover, the scaling factors κ_j in Eqn (4) are adapted to the use of projection angles α and β (Fig. 1) by setting $\kappa_0 = \cos\alpha\cos\beta$, $\kappa_1 = \sin\alpha\cos\beta$ and $\kappa_2 = \sin\beta$.[30]

Hence, the projection formalism of PR NMR is equivalent to the GFT NMR formalism. Several algorithms have been proposed for reconstructing the multidimensional spectrum,[30,33,34] but the extent to which the reconstruction introduces spectral artefacts remains a matter of debate.[30,33–37]

G^2FT NMR spectroscopy

The principle of GFT NMR can be applied twice for two distinct sets of chemical shifts, with each set being jointly sampled. This concept resulted in the introduction of G^2FT NMR spectroscopy.[38] In particular, efficient resonance assignment of polypeptide chemical shifts can be achieved by separate joint sampling of (i) chemical shifts that solely serve to provide increased resolution in one GFT dimension and (ii) shifts that also provide sequential connectivities in a second GFT dimension.

Survey of GFT NMR experiments

Table 1 provides a survey of published GFT/G^2FT NMR experiments thus far, which were named as such in the literature. Briefly, if an *N*D FT-NMR experiment is acquired as an $(N, N-K)$D GFT (or G^2FT) NMR experiment, $K+1$ chemical shifts are measured in a single (or two) 'GFT dimension(s)' in which *linear combinations* of the jointly sampled shifts are detected phase sensitively. The remaining frequency axes in the resulting $(N-K)$D subspectra are sampled as in conventional NMR. To indicate which chemical shifts are jointly sampled, the corresponding nuclei are underlined in the name of the experiments. Evidently, a large array of experiments have been developed for efficient resonance assignment and collection of NOE distance constraints. The highest dimensional spectral information that has so far been acquired for a globular protein is encoded in a (6,3)D $\underline{H}^{\alpha\beta}\underline{C}^{\alpha\beta}\underline{C}^{\alpha}\underline{CO}NHN$ GFT NMR experiment, which was recorded for the 76-residue protein ubiquitin.[13] Notably, automated peak picking of GFT NMR spectra profits greatly from the fact that chemical shift multiplets are detected. This allows one to employ pattern recognition algorithms for signal identification.[39]

Furthermore, several researchers have designed experiments that are closely related to GFT NMR experiments, or have used the GFT NMR approach for reconstruction of multidimensional spectra.[15,27–30,33–37,43–53] However, the rather nonuniform nomenclature used for the experiments impedes facile comparison. Hence, we have 'translated' the various names into those following the convention adopted for GFT NMR as described above. Table 2 provides a survey of GFT-type experiments, and it is apparent that a variety of novel innovations have been introduced. Among those, very recently published APSY[51] and HIFI[37] NMR are outstanding contributions toward integrated and fully automated projection NMR spectroscopy.

CONCLUSIONS

GFT NMR spectroscopy is an attractive solution for the 'NMR sampling problem'.[1] Its use in our laboratory in the framework of Northeast Structural Genomics consortium (http://www.nesg.org) has yielded so far resonance assignments for 14 proteins, which are deposited in the BioMagResBank,[54] and 13 protein structures, which are deposited in the Protein Data Bank.[55] Furthermore, a recent high-throughput study[40] exemplified the remarkable potential of GFT NMR-based structural genomics.[56]

Acknowledgements

Our research is supported by the Protein Structure Initiative of the National Institutes of Health (U54 GM074958-01 and U54 GM075026-01) and the National Science Foundation (MCB 0075773). We thank our colleagues of the Northeast Structural Genomics Consortium (NESGC) and the New York Center for Membrane Protein Structure (NYCOMPS).

REFERENCES

1. Atreya HS, Szyperski T. *Methods Enzymol.* 2005; **394**: 78.
2. Szyperski T, Yeh DC, Sukumaran DK, Moseley HNB, Montelione GT. *Proc. Natl. Acad. Sci. U.S.A.* 2002; **99**: 8009.

3. Kim S, Szyperski T. *J. Am. Chem. Soc.* 2003; **125**: 1385.
4. Ernst RR, Bodenhausen G, Wokaun A. *Principles of Nuclear Magnetic Resonance in One and Two Dimensions*. Oxford University Press: Oxford, 1987.
5. Nagayama K, Bachmann P, Wuthrich K, Ernst RR. *J. Magn. Reson.* 1978; **31**: 133.
6. Aue WP, Karhan J, Ernst RR. *J. Chem. Phys.* 1976; **64**: 4226.
7. Bodenhausen G, Ernst RR. *J. Magn. Reson.* 1981; **45**: 367.
8. Szyperski T, Wider G, Bushweller JH, Wüthrich K. *J. Biomol. NMR* 1993; **3**: 127.
9. Szyperski T, Wider G, Bushweller JH, Wüthrich K. *J. Am. Chem. Soc.* 1993; **115**: 9307.
10. Szyperski T, Pellecchia M, Wüthrich K. *J. Magn. Reson., Ser. B* 1994; **105**: 188.
11. Brutscher B, Cordier F, Simorre JP, Caffrey M, Marion D. *J. Biomol. NMR* 1995; **5**: 202.
12. Kim S, Szyperski T. *J. Biomol. NMR* 2004; **28**: 117.
13. Atreya HS, Szyperski T. *Proc. Natl. Acad. Sci. U.S.A.* 2004; **101**: 9642.
14. Freeman R, Kupce E. *Concepts Magn. Reson. Part A* 2004; **23A**: 63.
15. Brutscher B, Morelle N, Cordier F, Marion D. *J. Magn. Reson., Ser. B* 1995; **109**: 238.
16. Marion D, Wüthrich K. *Biochem. Biophys. Res. Commun*. 1983; **113**: 967.
17. Szyperski T, Braun D, Fernandez C, Bartels C, Wüthrich K. *J. Magn. Reson., Ser. B* 1995; **108**: 197.
18. Szyperski T, Braun D, Banecki B, Wüthrich K. *J. Am. Chem. Soc.* 1996; **118**: 8146.
19. Löhr F, Rüterjans H. *J. Biomol. NMR* 1995; **6**: 189.
20. Ding KY, Gronenborn AM. *J. Magn. Reson.* 2002; **156**: 262.
21. Güntert P, Dotsch V, Wider G, Wüthrich K. *J. Biomol. NMR* 1992; **2**: 619.
22. Delaglio F, Grzesiek S, Vuister GW, Zhu G, Pfeifer J, Bax A. *J. Biomol. NMR* 1995; **6**: 277.
23. Bartels C, Xia TH, Billeter M, Güntert P, Wüthrich K. *J. Biomol. NMR* 1995; **6**: 1.
24. Keller R. *The Computer Aided Resonance Assignment Tutorial*. Cantina Verlag: Goldau, 2004.
25. Moseley HNB, Monleon D, Montelione GT. *Methods Enzymol.* 2001; **339**: 91.
26. Baumann R, Kumar A, Ernst RR, Wüthrich K. *J. Magn. Reson.* 1981; **44**: 76.
27. Kupce E, Freeman R. *J. Biomol. NMR* 2003; **27**: 383.
28. Kupce E, Freeman R. *J. Am. Chem. Soc.* 2003; **125**: 13958.
29. Kupce E, Freeman R. *J. Biomol. NMR* 2004; **28**: 391.
30. Kupce E, Freeman R. *J. Am. Chem. Soc.* 2004; **126**: 6429.
31. Deans DS. *The Radon Transform and Some of its Applications*. Wiley: New York, 1983.
32. Natterer F. *The Mathematics of Computerized Tomography*. Wiley: New York, 1986.
33. Coggins BE, Venters RA, Zhou P. *J. Am. Chem. Soc.* 2004; **126**: 1000.
34. Venters RA, Coggins BE, Kojetin D, Cavanagh J, Zhou P. *J. Am. Chem. Soc.* 2005; **127**: 8785.
35. Malmodin D, Billeter M. *J. Magn. Reson.* 2005; **176**: 47.
36. Malmodin D, Billeter M. *J. Am. Chem. Soc.* 2005; **127**: 13486.
37. Eghbalnia HR, Bahrami A, Tonelli M, Hallenga K, Markley JL. *J. Am. Chem. Soc.* 2005; **127**: 12528.
38. Atreya HS, Eletsky A, Szyperski T. *J. Am. Chem. Soc.* 2005; **127**: 4554.
39. Moseley HNB, Riaz N, Aramini JM, Szyperski T, Montelione GT. *J. Magn. Reson.* 2004; **170**: 263.
40. Liu GH, Shen Y, Atreya HS, Parish D, Shao Y, Sukumaran DK, Xiao R, Yee A, Lemak A, Bhattacharya A, Acton TA, Arrowsmith CH, Montelione GT, Szyperski T. *Proc. Natl. Acad. Sci. U.S.A.* 2005; **102**: 10487.
41. Eletsky A, Atreya HS, Liu GH, Szyperski T. *J. Am. Chem. Soc.* 2005; **127**: 14578.
42. Shen Y, Atreya HS, Liu G, Szyperski T. *J. Am. Chem. Soc.* 2005; **127**: 9085.
43. Xia YL, Zhu G, Veeraraghavan S, Gao XL. *J. Biomol. NMR* 2004; **29**: 467.
44. Kozminski W, Zhukov I. *J. Biomol. NMR* 2003; **26**: 157.
45. Kozminski W, Zhukov I. *J. Magn. Reson.* 2004; **171**: 186.
46. Kozminski W, Zhukov I. *J. Magn. Reson.* 2004; **171**: 338.
47. Bersch B, Rossy E, Coves J, Brutscher B. *J. Biomol. NMR* 2003; **27**: 57.
48. Kupce E, Freeman R. *J. Magn. Reson.* 2005; **172**: 329.
49. Coggins BE, Venters RA, Zhou P. *J. Am. Chem. Soc.* 2005; **127**: 11562.
50. Jiang L, Coggins BE, Zhou P. *J. Magn. Reson.* 2005; **175**: 170.
51. Hiller S, Fiorito F, Wüthrich K, Wider G. *Proc. Natl. Acad. Sci. U.S.A.* 2005; **102**: 10876.
52. Sun ZYJ, Hyberts SG, Rovnyak D, Park S, Stern AS, Hoch JC, Wagner G. *J. Biomol. NMR* 2005; **32**: 55.
53. Reardon PN, Spicer LD. *J. Am. Chem. Soc.* 2005; **127**: 10848.
54. Seavey BR, Farr EA, Westler WM, Markley JL. *J. Biomol. NMR* 1991; **1**: 217.
55. Berman HM, Westbrook J, Feng Z, Gilliland G, Bhat TN, Weissig H, Shindyalov IN, Bourne PE. *Nucleic Acids Res.* 2000; **28**: 235.
56. Montelione GT, Zheng DY, Huang YPJ, Gunsalus KC, Szyperski T. *Nat. Struct. Biol.* 2000; **7**: 982.